19

Nonlinear Optical Properties of Graphene and Carbon Nanotube Composites

Jun Wang[1a], Yu Chen[1b], Rihong Li[1a], Hongxing Dong[1a], Long Zhang[1a], Mustafa Lotya[2], Jonathan N. Coleman[2] and Werner J. Blau[2]
[1a]*Key Laboratory of Materials for High-Power Laser, Shanghai Institute of Optics and Fine Mechanics, Chinese Academy of Sciences*
[1b]*Key Laboratory for Advanced Materials, Department of Chemistry, East China University of Science and Technology*
[2]*School of Physics and the Centre for Research on Adaptive Nanostructures and Nanodevices (CRANN), Trinity College Dublin*
[1]*China*
[2]*Ireland*

1. Introduction

The rapid development of nanoscience and nanotechnology provides lots of new opportunities for nonlinear optics. A growing number of nanomaterials have been shown to possess remarkable nonlinear optical (NLO) properties, which promotes the design and fabrication of nano and nano-scale optoelectronic and photonic devices (Xia et al. 2003; Avouris et al. 2008; Hasan et al. 2009; Bonaccorso et al. 2010; Loh et al. 2010; Coleman et al. 2011). The wonderful carbon allotropes discovered in recent decades are the most representative products of nanotechnology: from 3D carbon nanoparticles (graphite), to 0D fullerenes, to 1D carbon nanotubes (CNTs), and then to 2D graphenes discovered most recently. Interestingly, all of these nano-carbons exhibit diverse NLO properties. For instance, carbon black suspensions show strong thermally-induced nonlinear scattering (NLS) effect and hence optical limiting (OL) for intense ns laser pulses (Mansour et al. 1992); fullerenes show large third-order optical nonlinearity and reverse saturable absorption (RSA) at certain wavelength band (Tutt et al. 1992); CNTs show ultrafast second- and third-order nonlinearities and saturable absorption (SA) in the near infrared (NIR) region (Hasan et al. 2009); and graphenes show ultrafast carrier relaxation time and ultra-broad-band resonate NLO response (Bonaccorso et al. 2010).

Optical limiting is an important NLO phenomenon, which can be utilized to protect delicate optical instruments, especially the human eye, from intense laser beams (Tutt et al. 1993). As shown in Fig. 1, ideally an optical limiter should strongly attenuate intense, potentially dangerous laser beams, while exhibiting high transmittance for low intensity ambient light. Generally speaking, there are two main mechanisms for passive OL: nonlinear absorption (NLA) and NLS. The former can be further divided into multi-photon absorption (MPA), RSA and free-carrier absorption (FCA). Up to date, numerous inorganic and organic materials, such as phthalocyanines (O'Flaherty et al. 2003; de la Torre et al. 2004), porphyrins

(Blau et al. 1985; Senge et al. 2007), organic dyes (He et al. 1995; He et al. 2008), metal nanoclusters (Sun et al. 1999; Wang et al. 2009), quantum dots (He et al. 2007), etc. have been found to possess OL response. Carbon-related nanomaterials are actually a main branch in the field of OL materials (Chen et al. 2007; Wang et al. 2009). It has been confirmed that fullerene shows RSA induced OL, and nanotubes and graphene show NLS induced limiting. However, the most important point is that the advantage of these carbon nanomaterials manifests themselves in tailorable chemical properties by binding functional materials, e.g., polymers, organic molecules and metal nanoparticles, forming versatile OL composites (Chen et al. 2007; Wang et al. 2009; Bottari et al. 2010).

The large surface energy of nanotubes imposes restrictions on the formation of individual nanotubes in most inorganic and organic solvents. For solubilized nanotubes, one can employ polymers or organic molecules to functionalize, covalently or noncovalently, the surface of nanotubes. In the same manner, pristine single- or few-layer graphene is also difficult to exist stably in many organic solvents. It is thus very significant to design and synthesize nanotube- and graphene-based solution-processed organic/polymeric materials, which is a key step for the development of viable nano-carbon OL devices (Chen et al. 2007; Wang et al. 2009).

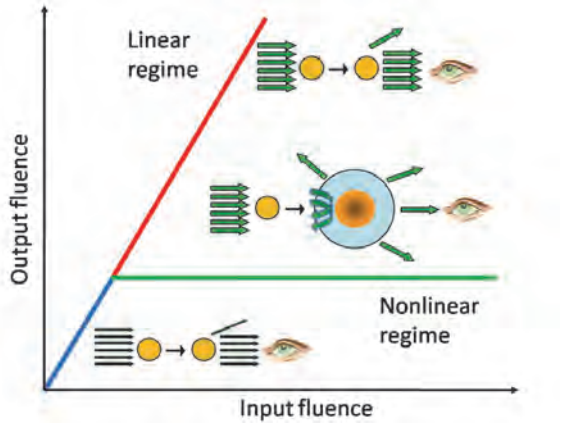

Fig. 1. The response of an ideal optical limiter.

2. Mechanisms

2.1 Nonlinear scattering (NLS)

Thermally induced NLS may be the most common nonlinear phenomenon for various nanomaterial systems, such as nanotubes, nanorods, nanowires, nanosheets, nanoribbons, nanospheres, nanodots etc. (Wang et al. 2009). An effective scattering process can disperse the highly intense beam into a larger spatial dimension and hence reduce the intensity of the direct incident beam. According to Mie scattering theory, the nanoscale particles alone cannot scatter a light beam effectively. The effective scattering arises from the formation of scattering centres with size of the order of the wavelength of the incident laser beam. The formation of scattering centres, initiating from nanoparticles, has three possible origins.

The induced scattering centres consist of two origins: the formation and growth of solvent bubbles, which is due to the thermal energy transfer from the nanotubes to the solvent; and

the formation and expansion of carbon microplasmas, which is due to the ionization of nanotubes. The former takes place at the lower incident energy fluence, while the latter takes place at higher fluences. Belousova et al. developed a theoretical model to explain the OL of carbon nanoparticles (Belousova et al. 2003; Belousova et al. 2004). In this model, the whole limiting process is described theoretically by three steps: the dynamics of the formation and expansion of solvent vapour bubbles; the Mie scattering of the expanding bubbles; and the nonlinear propagation through the scattering medium. Although the objects of modeling are quasi-spherical carbon nanoparticles, the Mie theory-based prediction works qualitatively for nanotubes and is helpful for understanding bubble growth dynamics and thus the OL process in CNT suspensions. As an example, Fig. 2a shows the variations of absorption and scattering cross sections as radius of gas bubbles in carbon nanoparticle suspensions, and Fig. 2b illustrates the inside pressure, expansion rate and radius of a gas bubble as functions of illumination time (Belousova et al. 2004). Moreover, Belousova's simulation indicates that the scattering cross section increases significantly with the increasing size of vapor bubbles, meanwhile the absorption cross section decreases until it is negligible when the bubbles grow, effectively limiting the incident power.

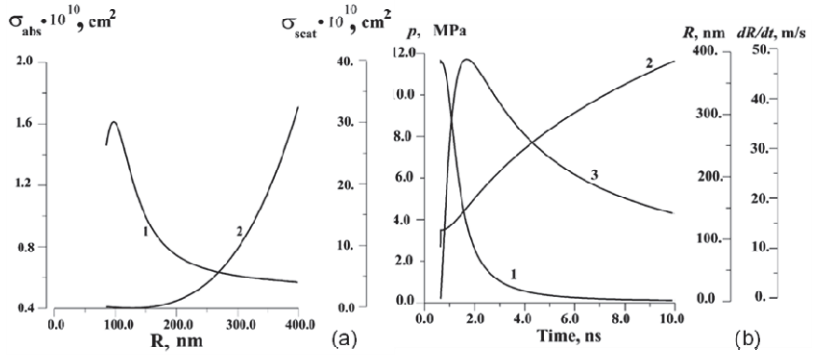

Fig. 2. Variations of (1) absorption and (2) scattering cross sections as radius of gas bubbles in carbon nanoparticle suspensions (a), and the inside pressure (1), expansion rate (2) and radius (3) of a gas bubble as functions of illumination time (b) (Belousova et al. 2004).

2.2 Reverse saturable absorption (RSA)

The process of RSA involves multi-step, excited state absorption (ESA) from the singlet ground state to the first excited triplet state via the first excited singlet state. The most representative materials include phthalocyanines, porphyrins, fullerenes, etc. A general five-level model, as shown in Fig. 3, has been considered to simulate the RSA process in the phthalocyanine system (O'Flaherty et al. 2003; O'Flaherty et al. 2004). The vibrational levels of the electronic states are ignored. Generally, for this five-level system after initial excitation, the first excited singlet state S_1 is populated, from here the electrons may be subsequently excited into S_2 within the pulse width of the laser. Once in S_2, they rapidly relax to S_1 again. From S_1, the population may undergo an intersystem crossing to the first excited triplet T_1 with a time constant τ_{isc} and thereafter undergo excitations and relaxations to and from T_2. Thus, the population is exchanged cyclically between S_1 and T_1, as the

lifetime of T_1 (τ_{ph}) is very long in comparison to τ_{isc}. With further simplify matters, it was assumed that relaxation out of states S_2 and T_2 is very rapid so that the population of these two levels may be neglected. Furthermore, stimulated emission from S_1 is excluded due to the small fluorescence quantum yield.

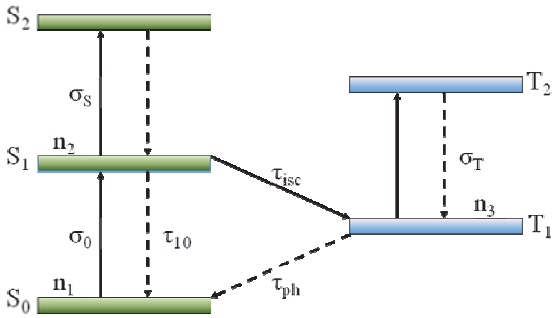

Fig. 3. Illustration of a five-level RSA process. Si represents singlet levels, and Ti represents triplet levels. Solid arrows imply an excitation resulting from photon absorption and dashed arrows represent relaxations.

The extinction of incident beam is governed by the propagation equation

$$\partial I/\partial z=-\alpha_{NL}I=-(\sigma_0N_1+\sigma_sN_2+\sigma_TN_3)I \quad (1)$$

where the nonlinear absorption coefficient α_{NL} is composed of the ground state absorption σ_0N_1, the first excited singlet state absorption σ_sN_2 and the first excited triplet state absorption σ_TN_3. N and σ refer to the population and absorption cross section of specific energy levels. Under the steady state approximation α_{NL} can be derived in the form,

$$\alpha_{NL}(F,F_{sat},\kappa)=\alpha_L(1+F/F_{sat})^{-1}(1+\kappa F/F_{sat}) \quad (2)$$

where α_L is the linear absorption coefficient, κ is the ratio of excited state cross section (σ_{ex}) to ground state cross section (σ_0), $\kappa=\sigma_{ex}/\sigma_0\approx\sigma_T/\sigma_0$, F represents the energy density and F_{sat} is the energy density at which the ground state absorption saturates (O'Flaherty et al. 2003; O'Flaherty et al. 2004). This model reproduces the RSA effects and highlights the crucial role that the ESA plays in the overall absorption coefficient. Considering this expression for the nonlinear absorption coefficient, one can state that higher κ values combined with lower F_{sat} values define more efficient OL ability.

2.3 Multi-photon absorption (MPA)

A multi-photon process is one which occurs through the simultaneous absorption of two or more photons via virtual states in a medium, as shown in Fig. 4. Many metals, semiconductor nanomaterials, quantum dots, organic chromophores and conjugated polymers possess multi-photon absorption induced OL effects (He et al. 2008). For two-photon absorption (TPA), the process can be described by a propagation equation with "Beer-Lambert" format

$$\partial I/\partial z=-(\alpha+\beta I)I \quad (3)$$

where α in unit of m^{-1} is the linear absorption coefficient and β in unit of m/W is the TPA coefficient. Provided that the linear absorption is very small at lower intensity, we obtain the solution for the transmission intensity

$$I(L)=I_0/(1+I_0\beta L). \quad (4)$$

It is clearly seen from the solution that the transmission intensity decreases as the incident intensity increases, resulting in OL phenomenon. The ability of TPA induced OL is strongly dependent on the TPA coefficient, the incident intensity, as well as the propagation length L. The TPA coefficient is related to the TPA cross section, a function of the exciting wavelength. The OL of TPA materials is more effective for shorter incident pulses, since the intensity of shorter pulses (ps or fs) is much higher than that of longer pulses (ns). The three-photon absorption process exhibits very similar characteristics.

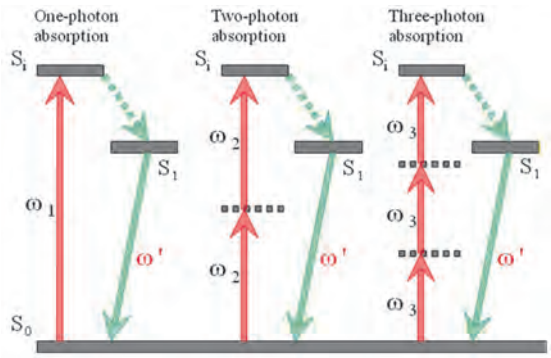

Fig. 4. Multi-photon absorption process.

In addition, it is worth discussing the difference of RSA and TPA processes under high intensity approximation. For RSA process, the nonlinear transmittance originates completely from the non-saturable ESA at very high intensities, hence tends to converge to a minimum transmittance T_{RSA}, which had been observed by Blau et al. in tetraphenylporphyrins in 1985 (Blau et al. 1985). The authors deduced analytically the expression for the minimum transmittance T_{RSA}, given by

$$T_{RSA}=T_0^{\kappa} \quad (5)$$

where $\kappa=\sigma_{ex}/\sigma_0$ is the ratio of excited state cross section (σ_{ex}) to ground state cross section (σ_0). Obviously, the minimum transmission for RSA is a non-zero quantity, which is dependent on κ, as well as the low intensity linear transmittance T_0. For TPA process, the transmitted intensity I(L) approaches a constant $1/\beta L$ at very high intensity $I_0 \rightarrow +\infty$, and hence the final transmittance $T_{TPA}=I(L)/I_0$ can reach to zero, resulting in a complete optical limitation. On the contrary, the RSA process theoretically cannot realize the complete limiting operation. Such difference between RSA and TPA is important for designing practical optical limiters.

2.4 Free-carrier absorption (FCA)

In semiconductors, carriers can be generated by one-photon or two-photon exciting. As shown in Fig. 5, these electron/hole pairs, by absorbing additional photons, can be excited

to states higher/lower in the conduction/valence band. The process is named 'free-carrier absorption', which is similar to ESA in molecular system (Boggess et al. 1986). It should be pointed out that there are four possible processes in a FCA medium – linear absorption, TPA, one-photon induced FCA and two-photon induced FCA. For the simplest case, the linearly excited one-photon induced FCA in Fig. 5 can be described by the propagation equation

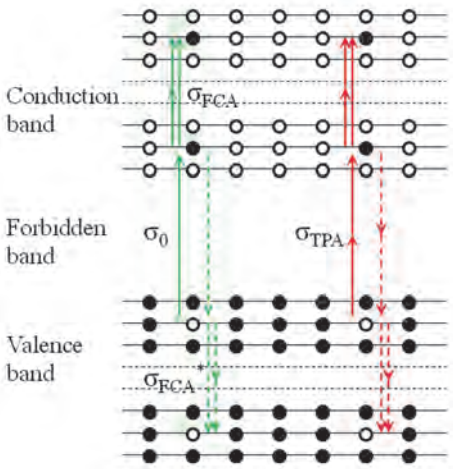

Fig. 5. Free-carrier absorption in semiconductor.

$$\partial I/\partial z=-(\alpha+\sigma_{FCA}N)I, \tag{6}$$

where σ_{FCA} is the FCA cross section. With the carrier density N given by $\partial N/\partial t=\alpha I/h\nu$, one can get an approximate solution for the propagation equation

$$T=T_0/[1+(1-T_0)(F_0\sigma_{FCA}/4h\nu)], \tag{7}$$

where T_0 is the linear transmission. When the peak incident fluence F_0 increases, the total transmission T decreases, resulting in an OL effect. For the most complicated case, all four processes take place in a FCA medium, then we have (Boggess et al. 1986; Tutt et al. 1993)

$$\partial I/\partial z=-(\alpha+\beta I^2+\sigma_{FCA}N)I \tag{8}$$

and

$$\partial N/\partial t=\alpha I/h\nu+\beta I^2/2h\nu. \tag{9}$$

A range of semiconductor nanoparticles, metal nanocomposites and quantum dotes exhibit FCA-induced OL effects. The FCA-induced NLO response is independent on the incident pulse duration, provided that the duration is shorter than the diffusion and recombination processes of free carriers. FCA is also insensitive to the particle size and geometry. It can work in both solid state films and suspensions, covering broad temporal and wavelength ranges. In many nanomaterials, FCA can coexist with NLS and TPA since the generation of free carriers can arise from a TPA process.

3. Graphene composites

Doubts about the stability of 2D crystals were finally dispelled by the discovery of graphene, a hexagonally symmetric, covalently bonded 2D carbon monolayer (Novoselov et al. 2004; Novoselov et al. 2005; Geim et al. 2007). Possessing excellent electronic properties, graphene provides a route to study fundamental quantum phenomena, such as the quantum hall effect in condensed-matter materials (Geim et al. 2007). Up to 10^5 $cm^2/V \cdot s$ mobility of charge carriers, which behave asmassless Dirac fermions in graphene, motivates the development of graphene-based electronic devices, challenging traditional silicon-based electronics (Geim et al. 2007).

In addition to the outstanding electronic, mechanical and thermal properties, graphene has been discovered to possess unique optical and photonic properties, which are summarized as follows.

1. The Dirac electrons in graphene have a linear dispersion between energy and momentum near the Dirac point, resulting in a continuously resonate optical response in a broadband spectral region from the visible to the near infrared (> 2.5 μm) (Geim et al. 2007).
2. Monolayer graphene shows wavelength independent linear optical absorption. For any low intensity light wave, the absorbance rigorously follows $\pi \cdot \alpha \approx 2.3\%$ per layer, where α is the fine-structure constant. As a result, the absorbance of multilayer graphene is proportional to the number of layers (Nair et al. 2008).
3. Graphene possesses ultrafast carrier dynamics due to the ultrafast carrier-carrier scattering and carrier-phonon scattering. Under the fs pulse excitation, the intraband equilibrium time is as short as ~100 fs and the intreband relaxation time is on a ps timescale (Dawlaty et al. 2008).
4. Graphene has significant NLO properties. Depending on the different experimental conditions, graphene and graphene oxide show NLS (Wang et al. 2009), ESA, TPA (Liu et al. 2009) or saturable absorption (SA) (Bao et al. 2009; Sun et al. 2010). Four-wave mixing experiment confirmed that the effective nonlinear susceptibility $|\chi^{(3)}|$ is as large as 10^{-7} esu in graphene flakes (Hendry et al. 2010). The second harmonic generation was also observed from a multi-layer graphene film (Dean et al. 2009).
5. Graphene oxide (GO) is a 2D network of mixed sp^2 and sp^3 carbon bondings. The isolated nanoscale sp^2 domains in the sp^3 matrix leads to a bandgap in GO. The width of the bandgap can be controlled by the size, shape and fraction of the sp^2 clusters, achieving a tunable photoluminescence and electroluminescence (Eda et al. 2010; Loh et al. 2010).

Before 2008, the study of photonic and optoelectronic properties of graphene have remained theoretical. With the help of development of the low-cost, high-yield method for mass production of graphene, the experimental study of NLO properties of graphene and graphene derivatives has developed very rapidly since 2009. Hereinafter, we introduce the NLO properties of graphene and its functionalized derivatives.

3.1 Graphene and graphene oxide

In contrast to micromechanical cleavage (Novoselov et al. 2005) and epitaxial growth (de Heer et al. 2007), a recently developed liquid-phase exfoliation technique provides a low-cost, high-yield method for mass production of unoxidized, defect-free graphene (Hernandez et al. 2008; Lotya et al. 2009). In this method, the sieved graphite powder was

dispersed in a range of organic solvents. After the low power sonication treatment and subsequent mild centrifugation to remove macroscopic aggregates, the homogeneous dark dispersions were obtained. All dispersions were stable against sedimentation and with only minimal aggregation occurring over a period of weeks. Experimental and theoretical analyses reveal that the surface energies of the selected solvents, e.g., N-methyl-2-pyrrolidone (NMP), N,N-dimethylacetamide (DMA), g-butyrolactone (GBL) etc., match very well that of graphite (~70–80 mJ m^{-2}), resulting in a minimal energy cost of overcoming the van der Waals forces between two graphene sheets, hence the effective exfoliation to graphene single or few layers (Bergin et al. 2008; Coleman 2009).

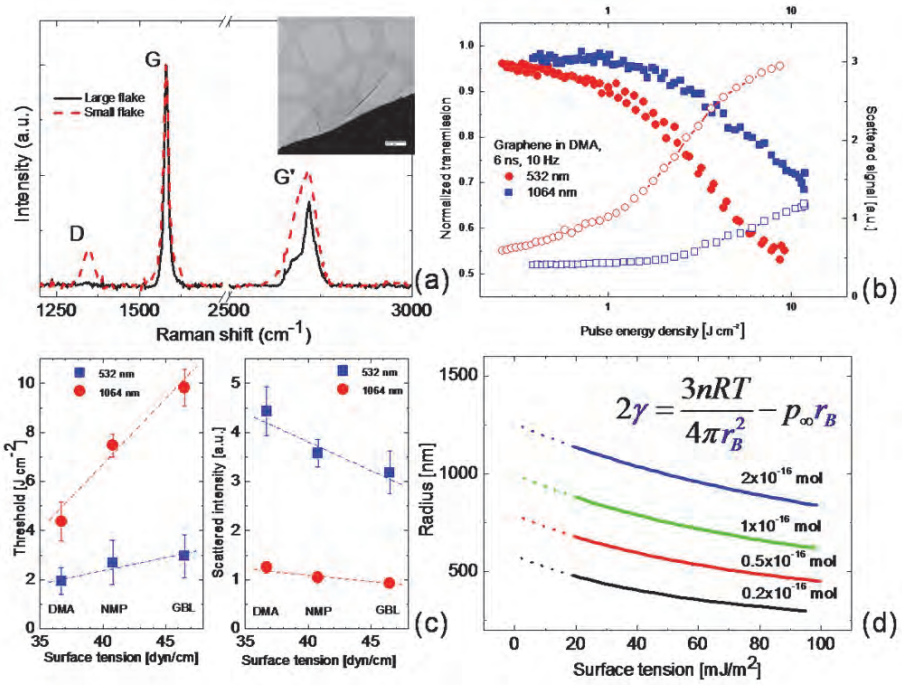

Fig. 6. TEM image, Raman spectra (a) and broadband OL (b) of the graphene dispersions. Limiting threshold and scattered intensity as functions of surface tension of solvents (c). Radius of the bubbles as a function of surface tension of solvents(d) (Wang et al. 2009).

Figure 6(a) show the TEM image and the Raman spectrum of graphene flakes prepared in γ-butyrolactone by the liquid-phase exfoliation technique. In addition to the clear TEM graph of the single-layer graphene flakes, the invisible D peak, as well as the clear G line and characterized 2D band, in the Raman spectrum witness the existence of defect-free monolayer and few-layer graphenes. We recently demonstrated that the liquid-phase exfoliated graphene dispersions exhibit broadband OL for ns pulses at 532 and 1064 nm, as shown in Fig. 6(b) (Wang et al. 2009). NLS, originating from the thermally induced solvent bubbles and microplasmas, is responsible for this nonlinear behaviour. The surface tension of the solvents has a strong influence on the OL performance of the graphene dispersions. As shown in Fig. 6(c), it is clear seen that the lower the surface tension, the smaller the

limiting threshold and the larger the scattered intensity. We established a simple model to estimate the radius of the gas bubbles as a function of the surface tension of the dispersant. The result in Fig. 6(d) reveals that the lower surface tension results in the larger bubble size, hence more effective scattering and OL. In addition, the graphene flakes exhibit a similar OL response to that of C_{60} and SWNTs.

Zhou et al. prepared a stable graphene solution by reducing GO using a simple and clean hydrothermal dehydration method, which can effectively remove oxygen-containing groups in GO and restore the aromatic rings (Zhou et al. 2009). The NLO properties of the reduced GO were measured by adsorbing the graphene on the end of an optical fiber, which guides a 1560 nm cw or 5 ns pulses laser beam for irradiation. The graphene exhibits a tunable NLA as well as OL response for the NIR light by changing the preparation conditions, i.e., temperature and pressure, and hence the oxygen functional groups and structural defects in graphene, which was confirmed by XPS, NMR and Raman spectroscopy.

The NLO properties of GO were studied by Liu et al. (Liu et al. 2009). Synthesized using the modified Hummers method, the GO was dispersed in DMF for the linear optical and NLO characterizations. UV-Vis spectrum of the GO dispersions shows an absorption peak at 268 nm, followed by a monotonously decreasing towards long wavelength region. Individual GO sheets were observed in AFM graph. The pulse open aperture Z-scan study verified that the RSA and TPA are mainly responsible for the NLO response of the GO solutions under ns and ps pulses at 532 nm, respectively. However, the contribution from NLS was not reported in Liu's paper. Feng et al. investigated the NLO and OL properties of a range of graphene derivatives, namely, graphene nanosheets, GO nanosheets, graphene nanoribbons and GO nanoribbons (Feng et al. 2010). Broadband NLO responses at 532 and 1064 nm were demonstrated in these graphene derivatives. Whereas the four derivatives exhibit different OL behavior, the NLS dominates the NLO response at 1064 nm while both the NLS and NLA contribute at 532 nm. Overall, the reduced graphenes possess better OL performance than the corresponding GO precursors due to the increased conjugation and crystallinity. The similar phenomenon was observed by Zhao et al., who found that the limiting response of graphene nanosheets is better than that of the GO nanosheets owing to the extended π conjugation in graphene (Zhao et al. 2010). In addition to the solvent dependent limiting properties studied, broadband limiting effect was realized as well using graphene nanosheets, which exhibit promising limiting at 532, 730, 800 and 1300 nm.

As with CNTs, the demonstration of graphene for OL renders graphene and related materials as a new class of nanomaterial for photonic and optoelectronic nanodevices (Bonaccorso et al. 2010). In the same way that nanotubes serve not only as nonlinear scatters but also as host material for functional counterparts, which we introduce below, this unique 2D nanomaterial could be a promising host for an optical limiter as well as for other photonic devices. Benefiting from the rich oxygen-containing groups, such as carboxyl and carbonyl groups on the edge and hydroxyl and epoxy groups on the basal plane, GO sheets can be decorated readily with a range of functional organic and inorganic materials by covalent or noncovalent combination, forming diverse nanohybrids with certain function (Loh et al. 2010).

3.2 Organic molecule functionalized graphene composites

For the NLO and OL applications, Xu et al. synthesized the first graphene hybrid by functionalizing with a metal-free porphyrin - TPP-NH_2. As shown in Fig. 7, the soluble graphene nanohybrid exhibits an improved OL performance compared with C_{60}, GO, TPP-NH2 and the mixture of the TPP-NH2 and GO (Xu et al. 2009). A more detailed NLO study reveals that the combination of multiple nonlinear mechanisms, i.e. RSA, TPA, NLS, as well

as photo-induced electron transfer results in the superior OL performance of the nanohybrid (Liu et al. 2009). The similar accumulation effect resulting in improved OL was confirmed in oligothiophene-graphene (Liu et al. 2009; Zhang et al. 2009) and fullerene-graphene (Liu et al. 2009; Zhang et al. 2009) nanohybrid systems as well. Very recently, the NLO properties of covalently linked graphene-metal porphyrins composite materials, namely, graphene-zinc porphyrin and graphene-copper porphyrins, were reported by Krishna et al. (Krishna et al. 2011). Effective combination of the different OL mechanisms, say, NLA, TPA, NLS and energy transfer in the graphene-porphyrin composites results in the improved OL effect for ns pulses at 532 nm. In the hybrid system, the existence of NLS, arising from the graphene moiety, can largely increase the damage threshold of the nano-composites. An energy transfer model based on the graphene-porphyrin hybrids was developed and verified that the energy transfer from porphyrin to graphene enhances the TPA of the system.

The role of energy transfer in the graphene based NLO materials was investigated by Mamidala et al., who blended the electron acceptor GO with positively charged porphyrin and negatively charged porphyrin, respectively (Mamidala et al. 2010). The NLO response of the positively charged porphyrin-GO system is much larger than that of the negatively charged porphyrin-GO system, confirming the important role of the energy transfer in such donor-acceptor complexes. While NLS dominates the OL effect, the energy transfer facilitates the deactivation of the hybrids, resulting in energy dissipation via the non-radiative decay and hence the effective heat accumulation in the hybrids or heat transfer from GO to the adjacent solvent. More pronounced energy transfer effect was seen in the porphyrin-Au nanoparticle complex, probably due to the better electron accepting ability of Au in comparison with the GO.

The analogous energy/electron transfer enhanced NLS was observed from a GO-dye ionic complex ($PNP^{+}GO^{-}$) (Balapanuru et al. 2010). Compared with the pristine GO and the dye PNPB, the charge-transfer composite exhibits much larger light scattering signal as well as nonlinear transmission and OL for ns pulses at both 532 and 1064 nm. The organic dye can effectively absorb the incident laser energy and transfer to the GO, resulting in the ionization of the GO or further transfer to solvent, forming microplasmas or vapor bubbles for NLS. From the above works, it should be pointed out that the energy transfer effect may inspire deeply the design and synthesis of the new OL hybrid materials.

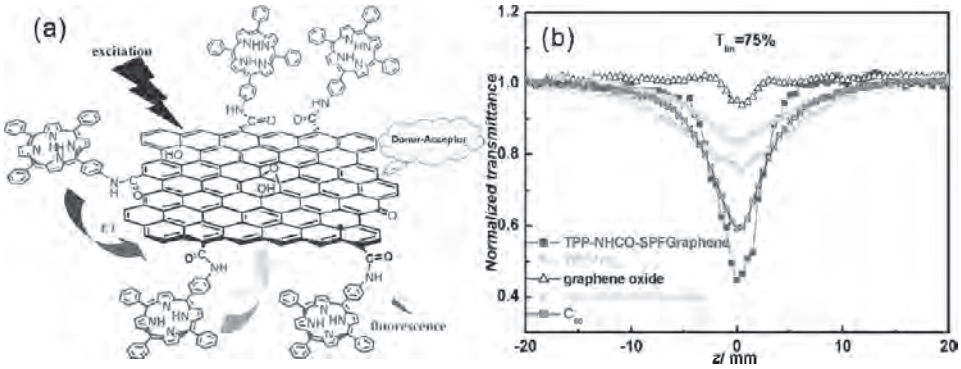

Fig. 7. The structure of the TPP-NH_2 functionalized GO (a) and the NLO response of the TPP-NH_2-GO compared with C_{60}, GO, TPP-NH2 and the mixture of the TPP-NH2 and GO (b) (Xu et al. 2009).

Very recently, we synthesized a soluble GO covalently functionalized with zinc phthalocyanine (PcZn), by an amidation reaction (Zhu et al. 2011). As shown in Fig. 8(a), the formation of an amido bond between PcZn and GO was confirmed by X-ray photoelectron and Fourier transform infrared spectroscopy. Fig. 8(b) presents the OL behavior of the GO-PcZn, GO and PcZn. It can be clearly seen that at the same level of linear transmission, GO-PcZn dispersions present much better OL performance than both GO and PcZn. As a result of the covalent link between GO and PcZn, The enhanced OL response at 532 nm can be attributed to the effective combination of the different NLO mechanisms, i.e., RSA of PcZn, and NLS and TPA of GO. It is likely that the significant scattering signal from the pure PcZn solution results from the formation of PcZn nanoparticles, as reported in []. Although PcZn did not make any significant contribution to the OL at 1064 nm [], it is surprising that the GO-PcZn dispersions have much greater OL response than GO. Coincidently, as shown in Fig. 8(b), the scattered curve from the GO-PcZn dispersions is steeper than that from GO as well. Whereas the origin of such large improvement of the OL at 1064 nm is not clear yet, it is possible that the energy transfer plays some role for the enhanced OL. After all, the GO-PcZn hybrid material has much better broadband NLO and OL performance than the GO alone.

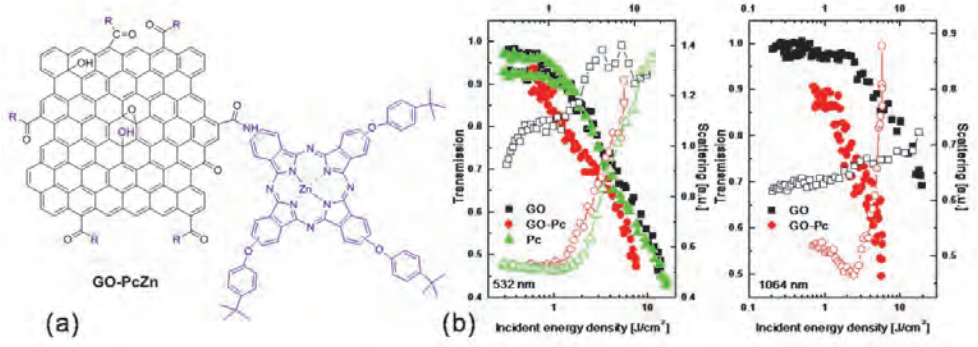

Fig. 8. The structure of the GO-PcZn composite (a) and the OL response of the GO-PcZn (b) (Zhu et al. 2011).

3.3 Polymer functionalized graphene composites

As mentioned above, graphene is insoluble in many organic solvents. To obtain solution-processed graphene polymer composites, the thermally-reduced graphene oxides (RGOs) were functionalized with poly(N-vinylcarbazole) (PVK) through generation of anions along the PVK backbone by using sodium hydride, followed by subsequent nucleophilic addition of these anionic species into the π-conjugated structure of the RGO platelets (Li et al. 2011). The structure of the RGO-PVK is depicted in Fig. 9(a). The wt% of RGO in the resulting polymer was estimated as 11.21%. Sonicated for 10 min in THF, the RGO-PVK dispersions are stable for at least one month (see Fig. 9(b)). Typical open aperture Z-scan results are depicted in Figs. 9(c) and 9(d). In contrast to PVK, which does not show any OL effect, the resulting hybrid material RGO-PVK displayed very good broadband NLO and OL responses at 532 and 1064 nm due to the effective combination of different NLO mechanisms, say, NLS and TPA.

Midya et al. synthesized a polymer functionalized RGO composite. The polymer used to covalently link with RGO is based on fluorene-thiophene-benzothiadazole as a donor-spacer-acceptor triad (Midya et al. 2010). With the good solubility in a range of common used organic solvents, the composite solution exhibits excellent OL performance for 532 nm ns pulses. With the help of the donor-acceptor electron transfer structure, the polymer-RGO hybrids show more effective NLS and hence OL than that of carbon nanotubes, RGO, or the polymer alone. However, the TPA from the polymer triads of the hybrids cannot be ruled out.

Aiming to the solid state NLO devices, Zhao et al. studied the OL response of graphene and GO nanosheets in a polymer gel matrix polyvinyl alcohol (PVA) (Zhao et al. 2010). The graphene-PVA composites exhibit a transparent and solid-like structure and possess remarkable OL effect for ns pulses at 532 nm. Operated at 10 Hz pulses, the graphene-PVA matrix emerge bleaching and degradation of the limiting performance after the first a few shots. This issue can be fixed by melting the PVA at 60-80 ^{o}C to rehomogenize the graphene in gel.

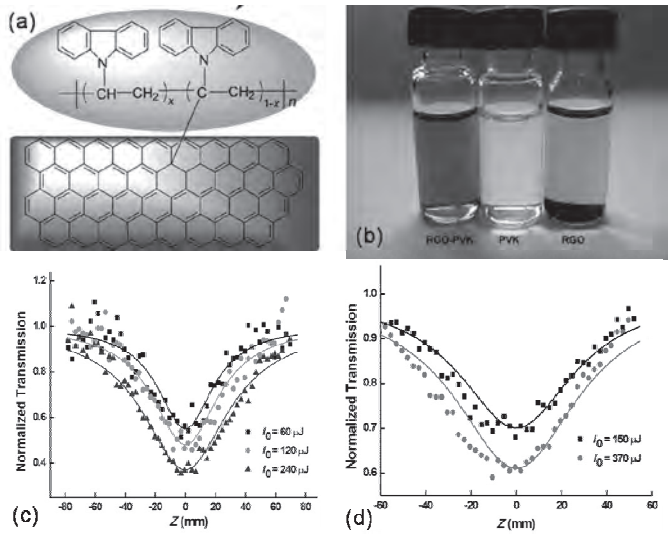

Fig. 9. The structure (a) and the solubility (b) of the RGO-PVK composite. The NLO responses of the RGO-PVK at 532 nm (c) and 1064 nm (d) (Li et al. 2011).

3.4 Nanostructure functionalized graphene composites

The linking of inorganic nanostructures on graphene nanosheets can result in the breakage of the electronic and molecular structures and the extended π conjugation of the graphene, and hence lower the device performance. Recently, Feng et al. developed a facile approach to preserve the lossless formation of graphene composite, in which the graphene was decorated with CdS quantum dots (QDs) by using benzyl mercaptan (BM) as the interlinker (see Fig. 10(a)) (Feng et al. 2010). TEM image reveals that the ~3 nm diameter CdS QDs are distributed uniformly on the surface of graphene nanosheets. As shown in Fig. 10(b), the CdS-graphene composite possesses outstanding broadband OL properties, mainly due to

NLS and FCA, for 532 and 1064 nm ns pulses. However, the energy transfer from the QDs to graphene cannot be ruled out. In addition, a Fe_3O_4 nanoparticles functionalized GO composite for OL was reported by Zhang et al. (Zhang et al. 2010).

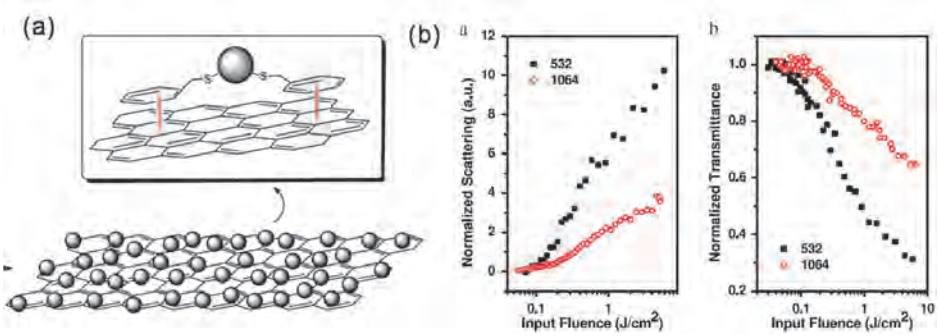

Fig. 10. The structure (a) and broadband OL (b) of the CdS-graphene composite (Feng et al. 2010).

4. Carbon nanotube composites

As 1D nanostructured materials, CNTs have attractive mechanical, electrical, and thermal properties, which have found many potential applications in the field of nanoscience and nanotechnology. In the past decade, CNTs have been extensively studied as an OL material (Chen et al. 2007; Wang et al. 2009). It is appealing that the nanotubes combine the advantages of the other two allotropes - carbon black has broadband OL and the fullerene acts as a favourable counterpart for functional materials. CNTs exhibit a significant OL effect covering a broad wavelength range from the visible to the NIR. Most importantly, the tailorable chemical properties of CNTs promote the synthesis of versatile nanotube composites by binding functional materials, e.g. metal nanoparticles, organic molecules and polymers.

4.1 Carbon nanotubes

Following the investigation of carbon black suspensions for OL, people started to realize that the CNT could be a new class of carbon nanomaterial for OL in 1998. Sun et al. and Chen et al. reported for the first time the OL property of nanotube suspensions (Sun et al. 1998; Chen et al. 1999). The broadband OL response was demonstrated using ns laser pulses and NLS was proposed as the primary mechanism for OL. In addition, the wavelength, solvent and bundle size effects were considered in their works. Vivien et al. studied systematically the OL performance, dynamics and mechanism of CNT suspensions by employing a series of experimental methods, e.g. Z-scan, the time-resolved pump-probe technique, white light emission measurement, the nonlinear transmittance experiment and the shadowgraphic imaging technique (Vivien et al. 1999; Vivien et al. 2000; Vivien et al. 2002; Vivien et al. 2002). Solvent bubble growth and the phase transition of CNTs at a range of incident fluences were observed, which confirmed that NLS, arising from solvent bubble and carbon vapour bubble formation, dominates the NLO properties of CNT suspensions. The impact of the incident beam wavelength and pulse duration on the OL performance has been studied as well. As described in subsection 2.1, one can simulate the growth dynamics of these bubbles in suspensions.

CNTs tend to aggregate into large bundles due to the high surface energy, which is a serious obstacle when it comes to real-life applications. People have found that CNTs can exist stably as individual nanotubes or small bundles in a range of amide solvents for reasonable periods of time. A typical example is the demonstration of large-scale debundling of single-walled nanotubes (SWNTs) by diluting nanotube dispersions with the solvent Nmethyl-2-pyrrolidinone (NMP) (Giordani et al. 2006). Experimental and theoretical analyses reveal that the surface energies of NMP and some other solvents, i.e. N,N-dimethylacetamide (DMA) and N,N-dimethylformamide (DMF) match very well with that of the nanotube. This results in a minimal energy cost to overcome the van der Waals forces between two nanotubes, and hence the effective debundling (Coleman 2009).

In recent years, we carried out a series of fundamental research on the OL mechanism, performance and its influence factor of the SWNT dispersions. The NLO properties of individual nanotubes were investigated in NMP, where the population of individual nanotubes was observed to increase as the concentration is decreased, with up to ~70% of all dispersed objects being individual nanotubes at a concentration of 4.0×10^{-3} mg ml^{-1} (Wang et al. 2008). AFM measurements reveal that the root-mean-square diameter of nanotubes decreases to less than 2 nm at 8.0×10^{-3} mg ml^{-1} before saturating at this level. Figure 11(a) shows the linear and NLO coefficients, deduced by open aperture Z-scan, as functions of the concentration of the SWNT dispersions in NMP. As the concentration of SWNTs is increased, the nonlinear extinction and OL effects improve significantly, while the limiting thresholds decrease gradually. Even with smaller sizes, the individual nanotubes still exhibit superior OL performance for 532 nm ns pulses than phthalocyanine nanoparticles and $Mo_6S_{4.5}I_{4.5}$ nanowires. The inset of Fig. 11(a) shows the difference between NLS-dominated nanotubes and RSA-dominated phthalocyanines. The nonlinear transmission of the SWNT dispersions has a distinct discontinuity, corresponding to a limiting threshold. The transmission is roughly constant when the energy fluence is below the threshold. When the incident fluence exceeds the threshold, the transmission decreases significantly. The limiting threshold implies that the nanotubes transfer enough heat energy to the surrounding solvent to cause the solvent to vaporize and grow to the critical size, in order to effectively scatter the incident beam. In contrast, the transmission of the phthalocyanines decreases with increasing incident energy. There is no evidence of the limiting threshold for phthalocyanines in the figure. Moreover, improved OL performance was found from the same nanotubes in DMF (Wang et al. 2008). As shown in Fig. 11(b), the DMF dispersions show superior nonlinear extinction effects and lower limiting thresholds. The static light scattering results in the inset of Fig. 11(b) proved that the DMF dispersions have the larger average bundle size, which in combination with the lower boiling point and surface tension of DMF, results in the superior optical limiting performance.

On the other hand, we showed that the OL performances of SWNT dispersions in NMP were enhanced significantly by blending a range of organic solvents or by increasing the temperature of the dispersions up to 100 ^{o}C (see Fig. 11(c) and 11(d)). While both nanotube bundle size and various solvent parameters have an influence on the OL responses, we verified experimentally that the surface tension of the solvent plays a more important role than the viscosity or boiling point; the appropriate solvent properties contribute to the NLS dominated OL phenomenon more than the bundle size (Wang et al. 2010). As the appropriate thermodynamic properties of the solvents are much more important for improving the OL performance, the solvent parameters were controlled by either changing the temperature of the dispersions or blending a secondary solvent (Wang et al. 2010). While

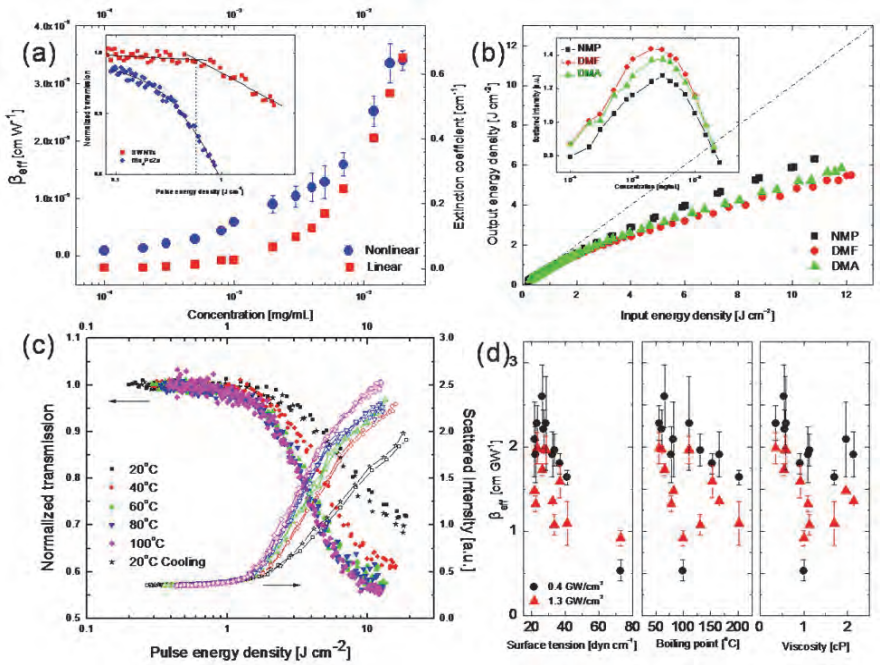

Fig. 11. The linear and NLO coefficients of the individual nanotube dispersions in NMP (a) (Wang et al. 2008). The OL of the nanotubes in different solvents (b) (Wang et al. 2008). The OL of the nanotube dispersions as a function of temperature (c) (Wang et al. 2010). Nonlinear extinction coefficient of the nanotube dispersions as a function of surface tension, boiling point and viscosity of the binary solvent mixtures (d) (Wang et al. 2010).

Effects on optical limiting		Optical limiting response
Structure of CNTs	SWNT, MWNT	SWNT ≈ MWNT
	Bundle diameter	The larger > The smaller
	Length	The longer ≥ The shorter
	Aspect ratio	The larger > The smaller
	Number density	The denser > The sparser
Physical properties of dispersant	Boiling point	The higher < The lower
	Surface tension	The larger < The smaller
	Viscosity	The higher < The lower
Laser source	Wavelength	The longer < The shorter
	Pulse duration	The longer > The shorter
	Repetition rate	The higher < The lower

Table 1. Summary of the factors that influence the OL responses of CNT dispersions. The signs of inequality indicate the contrast of OL responses.

the OL performance can be varied freely by increasing or decreasing the temperature from room temperature to 100 °C, the reduction of temperature below the freezing point of NMP and then down as far as -80 °C has little influence on the limiting performance. As a result of adding a small amount of organic solvent into the NMP dispersions, the NLO responses were enhanced significantly due to the reduction of surface tension and other parameters, as shown in Fig. 11(d). By contrast, the addition of water leads to a decrease in the optical limiting response. Nanotube dispersions in water/surfactant exhibit a similar limiting performance to the nanotubes in NMP. Our results reveal that the OL performance of the nanotube dispersions can be engineered by adjusting the solvent properties. Because the CNT dispersions are typical of the thermally induced light scattering dominated OL materials, we believe the conclusions fit not only the nanotubes but also other nanomaterials with the similar limiting mechanism.

4.2 Organic molecule functionalized nanotube composites

Most of the OL studies on pristine nanotubes concentrate on the physical mechanism and its influencing factors as summarized in Table 1. Although pristine nanotubes possess broadband limiting effects, the nanotubes alone could not satisfy all requirements for laser protection. The development of complex CNT composites is expected to enable practical OL devices. Whereas a lot of organic dyes exhibit NLA at certain wavelength bands, the optical limiting effect in nanotubes covers a broad wavelength range from the visible to the NIR. Nonlinear absorbers, i.e. phthalocyanines, have a quick response time in the ps regime, while nanotubes generally respond at best in the ns regime. Merging the complementary temporal and spatial nonlinear characteristics of NLA compounds and nanotubes has resulted in the development of nonlinear absorber-CNT hybrids by covalent or noncovalent link.

A TPA chromophore, Stilbene-3, and a SWNT mixture was prepared by Izard et al. (Izard et al. 2004). The cumulative OL effect was observed when the two moieties have comparable OL responses. If one moiety dominates, the whole limiting performance is close to that of the moiety. The composites, which exhibit both NLS and TPA, are expected to work in a broad temporal and spectral range. Webster et al. blended a RSA dye, 1,10,3,3,30,30-hexamethylindotricarbocyanine iodide (HITCI), with functionalized nitrogen-doped multi-walled nanotubes (MWNTs) to enhance the nonlinear transmittance of the whole system (Webster et al. 2005). The blended composite exhibits an improvement in the OL performance in comparison with the two individual materials. At the low intensity regime, the nonlinear response is dominated by the RSA dye HITCI before the NLS becomes significant. After the onset of NLS at the high intensity regime, nanotubes dominate the optical limiting. Blau and co-workers demonstrated the superior optical limiting effect from a noncovalently linked tetraphenylporphyrin–nanotube composite (Ni Mhuircheartaigh et al. 2006). The transmission electron microscope (TEM) image in Fig. 12(a) shows clearly the adhesion of porphyrin molecules to the outside of double-walled nanotubes by van der Waals interaction. The photo-induced electron transfer effects from covalently or noncovalently linked RSA dye-nanotube composites have been widely studied, which may help to improve the NLO response of such complex material systems. Recently, we reported the linear and NLO properties of a range of phthalocyanine-nanotube blends (see the inset of Fig. 12(b)) (Wang et al. 2008). The addition of nanotubes did not change the linear UV-visible absorption characteristics of phthalocyanines but resulted in significant fluorescence quenching. Due to the solvent effect, the phthalocyanine-nanotube composites in DMF

exhibit a larger nonlinear response than those in NMP. As shown in Fig. 12(b), the blends enhanced the OL performance in the higher energy density region when compared to the phthalocyanine solutions. In agreement with Webster et al.'s result, phthalocyanines influenced the OL effect in the lower energy density region, while the nanotubes played a more critical role in the attenuation of incident laser light in the higher energy density region. Overall, the OL behavior of the composites was increased with further addition of nanotubes.

Apart from the noncovalently-linked dye-nanotube composites, de la Torre et al. described the synthesis and characteristics of covalently functionalized single-walled nanotubes with metallophthalocyanines (de la Torre et al. 2003). Liu et al. synthesized covalently linked porphyrin-SWNT composites (Liu et al. 2008). The structures of the porphyrin-functionalized nanotubes are illustrated Fig. 12(c). Compared with C_{60}, individual nanotubes and porphyrins, the composite solutions show outstanding optical limiting responses for ns laser pulses at 532 nm. The authors attributed the superior performance to the effective combination of the NLO mechanism and the photo-induced electron transfer between porphyrins and nanotubes.

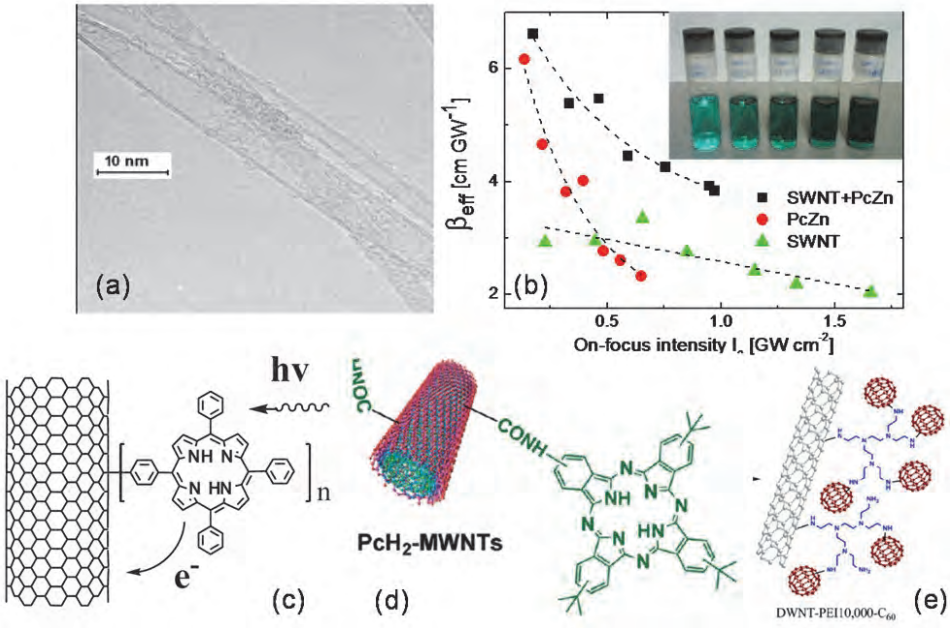

Fig. 12. TEM image showing the adhesion of organic porphyrin molecules to the outside of DWNT (a) (Ni Mhuircheartaigh et al. 2006). The nonlinear extinction coefficient as a function of on-focus intensity for various phthalocyanine–nanotube composites in DMF (b) (Wang et al. 2008). The structures of the porphyrin-SWNT (c) (Liu et al. 2008), PcH_2-MWNT (d) (He et al. 2009) and DWNT-C_{60} (e) (Liao et al. 2010).

Chen and his coworkers synthesized an unsymmetrically substituted metal-free phthalocyanine-covalently functionalized MWNT (PcH_2-MWNT) hybrid composite, in

which the wt % of MWNTs in the resulting product was found to be 35% (He et al. 2009). The molecular structure is given in Fig. 12(d). A considerably quenching of the fluorescence intensity was found in the photoluminescence spectrum of PcH_2-MWNTs. This observation suggests a quenching of the singlet excited PcH_2 by the covalently linked MWNTs. This material exhibits strong scattering at higher intensities, which evidently comes from the MWNT counterpart. The nonlinear response of PcH_2 is due to RSA, while that of PcH_2-MWNTs is due to both RSA and NLS, which could be two conflicted mechanisms for OL, giving rise to suppression of the whole nonlinear response of PcH_2-MWNTs.

Liao et al. synthesized a double-walled nanotube-fullerene (DWNT-C_{60}) hybrid by covalently linking DWNT and C_{60} by amination reaction with polyethylenimine (see Fig. 12(e)) (Liao et al. 2010). The nanohybrid can be dispersed in poly(m-phenylenevinylene-co-2,5-dioctoxy-p-phenylenevinylene) (PmPV) toluene solutions via 20 min sonication treatment. Both the hybrid dispersions and the polymer composites exhibit promising limiting effect, while the former works better due to the solvent effect discussed above. When dispersed in PmPV or chlorobenzene, the nanohybrid is expected to merge complementary temporal and spatial NLO characteristics of fullerene and CNTs, resulting in an enhanced OL. The OL performance of the DWNT-C_{60} hybrids is superior to those of C_{60} and SWNTs at the same level of transmission (~80%). Whereas NLS is an evident mechanism, RSA from C_{60} moieties has significant contribution. Photo-induced charge transfer between the DWNT and C_{60} moieties may also play an important role on the enhanced OL.

4.3 Polymer functionalized nanotube composites

As we mentioned above, nanotubes tend to aggregate into large bundles in most inorganic and organic solvents because of their relatively high surface energy, which is a serious obstacle when it comes to real-life applications. It is thus of great interest to design and prepare soluble nanotubes, which allows the easy manufacture of large-area thin film optoelectronic devices by spin coating or screen-printing technologies. Covalently or noncovalently functionalizing the surface of nanotubes by polymers is a simple and low-cost method to produce soluble nanotube and graphene composites.

A breakthrough in exploring the noncovalent interaction of the nanotube and polymer was made by Curran et al. who adopted a conjugated polymer, PmPV (see Fig. 13(a)), to disperse and purify the nanotubes, resulting in property modified nanocomposites (Curran et al. 1998). The coiled polymer conformation allows it to surround the layers of the nanotubes, permitting sufficiently close intermolecular proximity for π-π interaction to occur. The PmPV has a bright yellow color while the PmPV-nanotube composite possesses a deep green color, implying the strong interaction between the polymer chains and the nanotubes. As shown in Fig. 13(b), a clear wrapping effect of individual nanotubes by the PmPV matrix was observed by TEM. PmPV is an appropriate polymer to disperse CNTs while retaining the superior optical response from the nanotubes. O'Flaherty et al. prepared two kinds of polymer-nanotube composite by dispersing nanotubes into PmPV and poly(9,9-di-n-octylfluorenyl-2,7′-diyl) (PFO), respectively (O'Flaherty et al. 2003; O'Flaherty et al. 2003). Both of these composite systems showed an excellent OL effect on ns laser pulses at 532 nm. The strong back and front scattered light signals, with characteristics of Mie scattering, indicate evidence of the NLS origin of OL.

For soluble nanotube polymer composites, the preparation procedure usually involves mixing nanotube dispersions with solutions of the polymer and then evaporating the

solvents in a controlled way. The solution mixing approach is limited to polymers that freely dissolve in common solvents. An alternative method for producing a homogeneous dispersion of nanotubes is to incorporate nanotubes into thermoplastic polymers at the temperature higher than the melting point of these polymers or, to in situ polymerize the suitable monomers, such as styrene, aniline, phenylacetylene, and other monomers in the presence of nanotubes. Hereinafter, we introduce several covalently functionalized nanotube polymer composites for optical limiting.

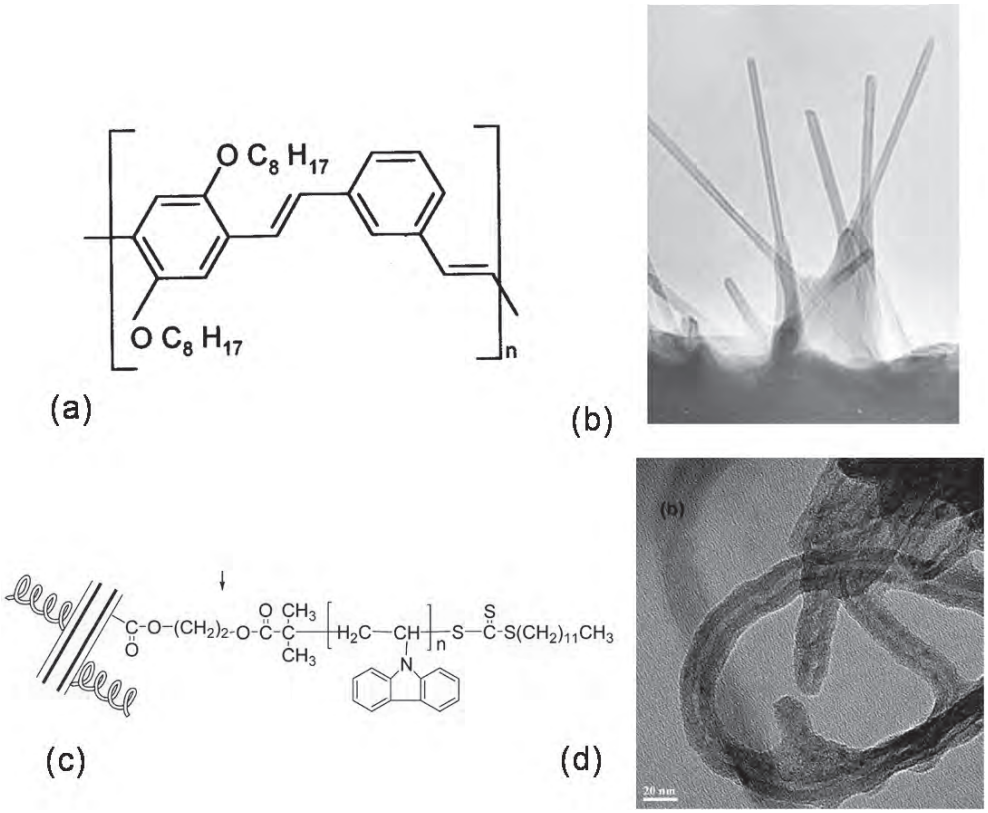

Fig. 13. The molecular structure of PmPV (a) and TEM image of nanotubes in PmPV (b) (Curran et al. 1998). The structure (c) and TEM image (d) of the MWNT-PVK hybrid (Zhang et al. 2010).

A series of poly(N-vinylcarbazole)-grafted MWNT (MWNT-PVK) hybrid materials were synthesized in the presence of S-1-Dodecyl-S′-(α, α′-dimethyl-α′′-acetic acid) trithiocarbonate (DDAT)-covalently functionalized MWNTs (MWNT-DDAT) as reversible addition-fragmentation chain transfer (RAFT) agent (Zhang et al. 2010). In that work, we used a new RAFT agent, DDAT-covalently functionalized MWNTs, first, and then grafted the PVK chains onto the surface of MWNTs to produce the soluble MWNT-PVK hybrid materials by RAFT polymerization, as shown in Fig. 13(c). High-resolution TEM graphs reveal that the MWNTs were coated by a layer of organic species whose thickness depends

on the molecular size and the quantity covalently attached onto the surface of MWNTs. The average diameter of MWNT-COOH is about 14 nm, while that of MWNT-PVK increases to 23-25 nm, as shown in Fig. 13(d). Incorporation of the PVK moieties onto the nanotube surface can considerably improve the solubility and processability of the nanotubes. For all MWNT-PVK hybrid materials, they are soluble in some common organic solvents such as toluene, THF, chloroform, DMF and others. At the same level of linear transmission, the MWNT-PVK with 79.2% PVK moieties in the material structure possesses best optical limiting performance for the ns pulses at 532 nm in comparison with the other MWNT-PVK composites, MWNTs and C_{60}. Light scattering, originating from the thermal-induced microplasmas and/or microbubbles, is responsible for the optical limiting. Subsequently, a new PVK-covalently grafted SWNT (SWNT-PVK) hybrid material was synthesized via an in situ anionic polymerization reaction of N-vinylcarbazole and the negatively charged SWNTs (Li et al. 2011). Same as the MWNT-PVK, appearance of the PVK moieties onto the surface of nanotubes significantly improves the solubility and processability of the SWNTs. At the same level of linear transmission, the SWNT-PVK dispersions show better optical limiting performance than the pristine SWNT dispersions. Micro-plasma and/or micro-bubble induced NLS is considered as the main mechanism for the OL.

In addition to the non-conjugated polymer, i.e., PVK, we also adopt conjugated polymer to functionalized covalently nanotubes. A new conjugated polymer PCBF with pendent amino groups in the polymer side chains was synthesized by the Suzuki coupling reaction (Niu et al. 2011). Then, this polymer was used to react with MWNTs with surface-bonded acryl chloride moieties to give a soluble donor-acceptor type MWNT-PCBF hybrid material, in which PCBF was chosen as electron donor, whereas the MWNT itself may serve as the electron acceptor. The TEM graph implies that the average thickness of PCBF covalently grafted onto the MWNTs is around 10.4 nm. After the low power sonication treatment, the MWNT-PCBF in tetrahydrofuran (THF) is stable for at least one month at a concentration as high as 5 g/L. It can be clearly seen that MWNT-PCBF exhibited excellent optical limiting performance. The MWNT-PCBF manifests the remarkable broadband OL with a comparable limiting performance for both 532 and 1064 nm pulses. The strong scattering signals indicate that the thermally induced NLS is responsible for the OL.

4.4 Nanostructure functionalized nanotube composites

The optical properties of CNTs can be modified by coating functional composites. Chin et al. successfully improved the transmission of nanotubes in the near UV region by coating silicon carbide or silicon nitride on the surface (Chin et al. 2004). The high transmission nanotube composites incorporated with good OL performances are appropriate for the development of laser protection devices. The same authors further employed polycrystalline Au or Ag nanoparticles as coatings deposited on the outside of multi-walled nanotubes (Chin et al. 2005). Broadband OL effects for ns pulses at 532 nm and 1064 nm were demonstrated in the functionalized nanotube composites. Enhanced limiting performance for 532 nm pulses was observed from the composites when compared with pristine nanotubes. The surface plasmon absorption (SPA) of Au and Ag coatings at 532 nm is attributed to the enhancement of the NLS as well as the optical limiting effect in the nanotube composites. However, polycrystalline Ni- and Ti-coated nanotubes did not show significant improvement for optical limiting since Ni and Ti nanoparticles do not exhibit SPA around 532 nm. Moreover, it should be mentioned that the CNT and carbon

nanoparticle mixtures were studied as a class of optical limiting nanomaterial as well (O'Flaherty et al. 2003).

Recently, Zhan and her coworkers synthesized a MWNT composite by functionalizing the sidewalls of nanotubes with CdS QDs using a two-step approach, with in situ polymerized thiophene as interlinker (Feng et al. 2010). TEM, XRD and TGA analyses verified that the thiophene coating formed on the surface of the MWCNTs by means of π electron interactions and the subsequent coupling of CdS QDs. As a consequence of interparticle coupling and the low percentage of CdS in the MWNT-PTh-CdS, the absorption of CdS becomes weaker and broader. Strong PL quenching of the CdS was observed after bonding to the nanotubes due to electron/energy transfer from the excited CdS QDs to the nanotubes. The MWNT-PTh-CdS exhibit a remarkable OL enhancement in comparison with the pristine MWNTs, especially at 1064 nm, owing to the presence of CdS QDs linked by conducting PTh to the MWCNTs and the subsequent electron/energy transfer facilitated NLS.

The same authors further prepared a series of functionalized MWNT composites by coating different conducting, semiconducting, and insulating materials, i.e., crystalline Au nanoparticles, TiO_2 nanoclusters, and amorphous SiO_2 nanoshells, on the sidewalls of the nanotubes (Zheng et al. 2010). The synthesis employed a combination of self-assembly and sol-gel technique. The structures and the TEM images of the three composites are illustrated in Fig. 14. The composites with Au-, TiO_2-, and SiO_2-coatings exhibit respectively the superior, equivalent, and inferior OL performance in comparison with the pristine nanotubes. As discussed above, the distinct OL response is likely due to the different electron/energy transfer strength, which largely influences the NLS process. In the three coatings, the conducting Au nanoparticles show the most effective electron transfer to the metallic nanotubes, resulting in the best NLS and OL.

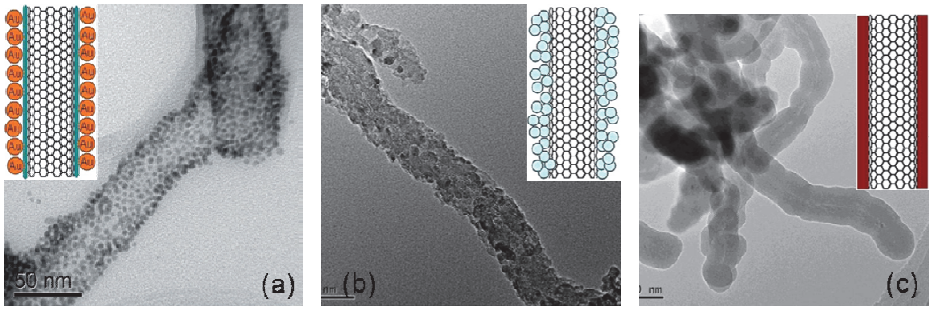

Fig. 14. The structures and TEM images of MWNTs functionalized with crystalline Au nanoparticles (a), TiO_2 nanoclusters (b) and amorphous SiO_2 nanoshells (c) (Zheng et al. 2010).

5. Summary and remarks

1. It is seen from the literature statistics in Fig. 15 using the *ISI Web of Science* that the development of OL keeps vigorously in recent decade. Especially, the involvement of nanotube and graphene invigorates this tendency. As we mentioned above, the excellent chemical activity of graphene and nanotubes provides a broad platform for various functional counterparts, forming multi-component, multi-functional hybrid composites with wider spatial and temporal responses for OL.

2. The derivatives of graphene and nanotube represent a key branch in the field of OL. In most of such nanohybrids, it is being attached importance to the electron/energy transfer from functional moiety to graphene or nanotube, which is considered playing an influential role on improving OL performance.
3. While the chemical synthesis and characterization of the OL materials develops rapidly, the corresponding NLO testing technique and theoretical analysis seems have reached a plateau. Merely a few papers report new measurement method or theoretical modelling for the OL materials (Belousova et al. 2003; Belousova et al. 2004; Venkatram et al. 2005; Gu et al. 2008; Rayfield et al. 2010). It is short of the NLO theory specific to the multi-component, multi-mechanism nanohybrids, which is probably the bottleneck restricts a ultimately improvement of the OL performance. The research of OL briefly consists of materials, mechanisms, the design of OL device. Aiming to industry capable OL devices, a balanced development of the three aspects is undoubtedly urgent.

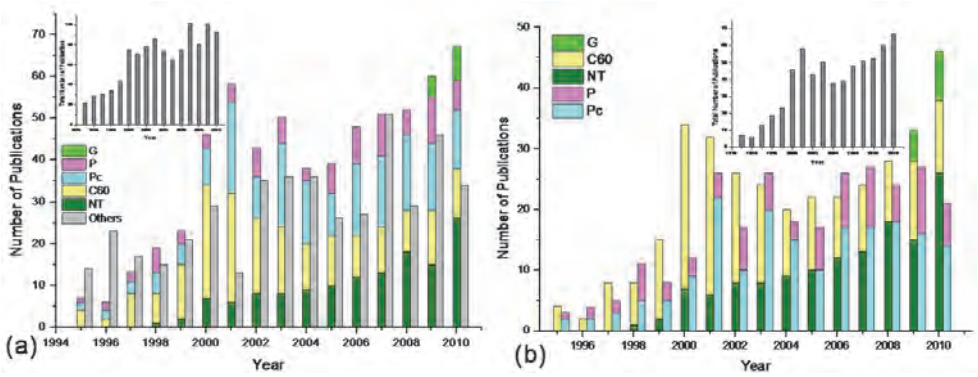

Fig. 15. A literature statistics using the *ISI Web of Science* restricted to the most plausible candidates for OL, namely, CNTs, graphene, C_{60}, phthalocyanines and porphyrins, shows an increasing trend in publications on CNTs, graphene, and their derivatives compared with other materials. Only original articles were included, review articles were excluded.

6. Acknowledgments

This work was supported by the starting grant of the 100-Talent Program of SIOM, Chinese Academy of Sciences (1108221-JR0) and the National Natural Science Foundation of China (50802103 and 51072207). Y.C. thanks for the financial supports of the National Natural Science Foundation of China (20676034 and 20876046), the Ministry of Education of China (309013), the Fundamental Research Funds for the Central Universities, the Shanghai Municipal Educational Commission for the Shuguang fellowship (08GG10) and the Shanghai Eastern Scholarship.

7. References

Avouris, P., M. Freitag and V. Perebeinos (2008). Carbon-nanotube photonics and optoelectronics. *Nature Photonics*, Vol. 2, No. 6, pp. 341-350.

Balapanuru, J., J. X. Yang, S. Xiao, Q. L. Bao, M. Jahan, L. Polavarapu, J. Wei, Q. H. Xu and K. P. Loh (2010). A Graphene Oxide-Organic Dye Ionic Complex with DNA-Sensing and Optical-Limiting Properties. *Angewandte Chemie-International Edition*, Vol. 49, No. 37, pp. 6549-6553.

Bao, Q., H. Zhang, Y. Wang, Z. Ni, Y. Yan, Z. X. Shen, K. P. Loh and D. Y. Tang (2009). Atomic-Layer Graphene as a Saturable Absorber for Ultrafast Pulsed Lasers. *Advanced Functional Materials*, Vol. 19, No.19, pp. 3077–3083.

Belousova, I. M., N. G. Mironova, A. G. Scobelev and M. S. Yur'ev (2004). The investigation of nonlinear optical limiting by aqueous suspensions of carbon nanoparticles. *Optics Communications*, Vol. 235, No. 4-6, pp. 445-452.

Belousova, I. M., N. G. Mironova and M. S. Yur'ev (2003). Theoretical investigation of nonlinear limiting of laser radiation power by suspensions of carbon particles. *Optics and Spectroscopy*, Vol. 94, No. 1, pp. 86-91.

Bergin, S. D., V. Nicolosi, P. V. Streich, S. Giordani, Z. Y. Sun, A. H. Windle, P. Ryan, N. P. Niraj, Z. T. Wang, L. Carpenter, W. J. Blau, J. Boland, J. P. Hamilton and J. N. Coleman (2008). Towards Solutions of Single-Walled Carbon Nanotubes in Common Solvents. *Advanced Materials*, Vol. 20, No. 10, pp. 1876-1881.

Blau, W., H. Byrne, W. M. Dennis and J. M. Kelly (1985). Reverse saturable absorption in tetraphenylporphyrins. *Optics Communications*, Vol. 56, No. 1, pp. 25-29.

Boggess, T. F., K. M. Bohnert, K. Mansour, S. C. Moss, I. W. Boyd and A. L. Smirl (1986). SIMULTANEOUS MEASUREMENT OF THE 2-PHOTON COEFFICIENT AND FREE-CARRIER CROSS-SECTION ABOVE THE BANDGAP OF CRYSTALLINE SILICON. *Ieee Journal of Quantum Electronics*, Vol. 22, No. 2, pp. 360-368.

Bonaccorso, F., Z. Sun, T. Hasan and A. C. Ferrari (2010). Graphene photonics and optoelectronics. *Nature Photonics*, Vol. 4, No.9, pp. 611-622.

Bottari, G., G. de la Torre, D. M. Guldi and T. Torres (2010). Covalent and Noncovalent Phthalocyanine-Carbon Nanostructure Systems: Synthesis, Photoinduced Electron Transfer, and Application to Molecular Photovoltaics. *Chemical Reviews*, Vol. 110, No. 11, pp. 6768-6816.

Chen, P., X. Wu, X. Sun, J. Lin, W. Ji and K. L. Tan (1999). Electronic structure and optical limiting behavior of carbon nanotubes. *Physical Review Letters*, Vol. 82, No. 12, pp. 2548-2551.

Chen, Y., Y. Lin, Y. Liu, J. Doyle, N. He, X. D. Zhuang, J. R. Bai and W. J. Blau (2007). Carbon nanotube-based functional materials for optical limiting. *Journal of Nanoscience and Nanotechnology*, Vol. 7, No. 4-5, pp. 1268-1283.

Chin, K. C., A. Gohel, W. Z. Chen, H. I. Elim, W. Ji, G. L. Chong, C. H. Sow and A. T. S. Wee (2005). Gold and silver coated carbon nanotubes: An improved broad-band optical limiter. *Chemical Physics Letters*, Vol. 409, No. 1-3, pp. 85-88.

Chin, K. C., A. Gohel, H. I. Elim, W. Ji, G. L. Chong, K. Y. Lim, C. H. Sow and A. T. S. Wee (2004). Optical limiting properties of amorphous SixNy and SiC coated carbon nanotubes. *Chemical Physics Letters*, Vol. 383, No. 1-2, pp. 72-75.

Coleman, J. N. (2009). Liquid-Phase Exfoliation of Nanotubes and Graphene. *Advanced Functional Materials*, Vol. 19, No. 23, pp. 3680-3695.

Coleman, J. N., M. Lotya, A. O'Neill, S. D. Bergin, P. J. King, U. Khan, K. Young, A. Gaucher, S. De, R. J. Smith, I. V. Shvets, S. K. Arora, G. Stanton, H. Y. Kim, K. Lee, G. T. Kim, G. S. Duesberg, T. Hallam, J. J. Boland, J. J. Wang, J. F. Donegan, J. C. Grunlan, G. Moriarty, A. Shmeliov, R. J. Nicholls, J. M. Perkins, E. M. Grieveson, K. Theuwissen, D. W. McComb, P. D. Nellist and V. Nicolosi (2011). Two-Dimensional

Nanosheets Produced by Liquid Exfoliation of Layered Materials. *Science*, Vol. 331, No. 6017, pp. 568-571.

Curran, S. A., P. M. Ajayan, W. J. Blau, D. L. Carroll, J. N. Coleman, A. B. Dalton, A. P. Davey, A. Drury, B. McCarthy, S. Maier and A. Strevens (1998). A composite from poly(m-phenylenevinylene-co-2,5-dioctoxy-p-phenylenevinylene) and carbon nanotubes: A novel material for molecular optoelectronics. *Advanced Materials*, Vol. 10, No. 14, pp. 1091-1093.

Dawlaty, J. M., S. Shivaraman, M. Chandrashekhar, F. Rana and M. G. Spencer (2008). Measurement of ultrafast carrier dynamics in epitaxial graphene. *Applied Physics Letters*, Vol. 92, No. 4, pp. 042116.

de Heer, W. A., C. Berger, X. S. Wu, P. N. First, E. H. Conrad, X. B. Li, T. B. Li, M. Sprinkle, J. Hass, M. L. Sadowski, M. Potemski and G. Martinez (2007). Epitaxial graphene. *Solid State Communications*, Vol. 143, No. 1-2, pp. 92-100.

de la Torre, G., W. J. Blau and T. Torres (2003). A survey on the functionalization of single-walled nanotubes: The chemical attachment of phthalocyanine moieties. *Nanotechnology*, Vol. 14, No.7, pp. 765-771.

de la Torre, G., P. Vaquez, F. Agullo-Lopez and T. Torres (2004). Role of structural factors in the nonlinear optical properties of phthalocyanines and related compounds. *Chemical Reviews*, Vol. 104, No. 9, pp. 3723-3750.

Dean, J. J. and H. M. v. Driel (2009). Second harmonic generation from graphene and graphitic films. *Applied Physics Letters*, Vol. 95, No. 26, pp. 261910.

Eda, G., Y. Y. Lin, C. Mattevi, H. Yamaguchi, H. A. Chen, I. S. Chen, C. W. Chen and M. Chhowalla (2010). Blue Photoluminescence from Chemically Derived Graphene Oxide. *Advanced Materials*, Vol. 22, No. 4, pp. 505–509.

Feng, M., R. Q. Sun, H. B. Zhan and Y. Chen (2010). Decoration of carbon nanotubes with CdS nanoparticles by polythiophene interlinking for optical limiting enhancement. *Carbon*, Vol. 48, No. 4, pp. 1177-1185.

Feng, M., R. Q. Sun, H. B. Zhan and Y. Chen (2010). Lossless synthesis of graphene nanosheets decorated with tiny cadmium sulfide quantum dots with excellent nonlinear optical properties. *Nanotechnology*, Vol. 21, No. 7, pp. 075601.

Feng, M., H. B. Zhan and Y. Chen (2010). Nonlinear optical and optical limiting properties of graphene families. *Applied Physics Letters*, Vol. 96, No. 3, pp. 033107.

Geim, A. K. and K. S. Novoselov (2007). The rise of graphene. *Nature Materials*, Vol. 6, No. 3, pp. 183-191.

Giordani, S., S. D. Bergin, V. Nicolosi, S. Lebedkin, M. M. Kappes, W. J. Blau and J. N. Coleman (2006). Debundling of single-walled nanotubes by dilution: Observation of large populations of individual nanotubes in amide solvent dispersions. *Journal of Physical Chemistry B*, Vol. 110, No. 32, pp. 15708-15718.

Gu, B., W. Ji, P. S. Patil, S. M. Dharmaprakash and H. T. Wang (2008). Two-photon-induced excited-state absorption: Theory and experiment. *Applied Physics Letters*, Vol. 92, No. 9, pp 091118.

Hasan, T., Z. Sun and A. C. Ferrari (2009). Nanotube–polymer composites for ultrafast photonics. *Advance Materials*, Vol. 21, No. 38-39, pp. 3874-3899.

He, G. S., J. D. Bhawalkar, C. F. Zhao and P. N. Prasad (1995). Optical limiting effect in a two-photon absorption dye doped solid matrix. *Applied Physics Letters*, Vol. 67, No. 17, pp. 2433-2435.

He, G. S., L. S. Tan, Q. D. Zheng and P. N. Prasad (2008). Multiphoton Absorbing Materials: Molecular Designs, Characterizations, and Applications. *Chemical Reviews*, Vol. 108, No. 4, pp. 1245-1330.

He, G. S., K. T. Yong, Q. D. Zheng, Y. Sahoo, A. Baev, A. I. Ryasnyanskiy and P. N. Prasad (2007). Multi-photon excitation properties of CdSe quantum dots solutions and optical limiting behavior in infrared range. *Optics Express*, Vol. 15, No. 20, pp. 12818-12833.

He, N., Y. Chen, J. Bai, J. Wang, W. J. Blau and J. Zhu (2009). Preparation and Optical Limiting Properties of Multiwalled Carbon Nanotubes with π-Conjugated Metal-Free Phthalocyanine Moieties. *Journal of Physical Chemistry C*, Vol. 113, No. 30, pp. 13029-13035.

Hendry, E., P. J. Hale, J. Moger, A. K. Savchenko and S. A. Mikhailov (2010). Coherent Nonlinear Optical Response of Graphene. *Physical Review Letters*, Vol. 105, No. 9, pp. 097401.

Hernandez, Y., V. Nicolosi, M. Lotya, F. M. Blighe, Z. Sun, S. De, I. T. McGovern, B. Holland, M. Byrne, Y. K. Gun'Ko, J. J. Boland, P. Niraj, G. Duesberg, S. Krishnamurthy, R. Goodhue, J. Hutchison, V. Scardaci, A. C. Ferrari and J. N. Coleman (2008). High-yield production of graphene by liquid-phase exfoliation of graphite. *Nature Nanotechnology*, Vol. 3, No. 9, pp. 563-568.

Izard, N., C. Menard, D. Riehl, E. Doris, C. Mioskowski and E. Anglaret (2004). Combination of carbon nanotubes and two-photon absorbers for broadband optical limiting. *Chemical Physics Letters*, Vol. 391, No. 1-3, pp. 124-128.

Krishna, M. B. M., V. P. Kumar, N. Venkatramaiah, R. Venkatesan and D. N. Rao (2011). Nonlinear optical properties of covalently linked graphene-metal porphyrin composite materials. *Applied Physics Letters*, Vol. 98, No. 8, pp. 081106.

Li, P.-P., Y. Chen, J. Zhu, M. Feng, X. Zhuang, Y. Lin and H. Zhan (2011). Charm-Bracelet-Type Poly(N-vinylcarbazole) Functionalized with Reduced Graphene Oxide for Broadband Optical Limiting. *Chemistry – A European Journal*, Vol. 17, No. 3, pp. 780-785.

Li, P. P., L. J. Niu, Y. Chen, J. Wang, Y. Liu, J. J. Zhang and W. J. Blau (2011). In situ synthesis and optical limiting response of poly(N-vinylcarbazole) functionalized single-walled carbon nanotubes. *Nanotechnology*, Vol. 22, No. 1, pp. 015204.

Liao, K.-S., J. Wang, D. Früchtl, N. J. Alley, E. Andreoli, E. P. Dillon, A. R. Barron, H. Kim, H. J. Byrne, W. J. Blau and S. A. Curran (2010). Optical limiting study of double wall carbon nanotube-fullerene hybrids. *Chemical Physics Letters*, Vol. 489, No. 4-6, pp. 207-211.

Liu, Y. S., J. Y. Zhou, X. L. Zhang, Z. B. Liu, X. J. Wan, J. G. Tian, T. Wang and Y. S. Chen (2009). Synthesis, characterization and optical limiting property of covalently oligothiophene-functionalized graphene material. *Carbon*, Vol. 47, No. 13, pp. 3113-3121.

Liu, Z. B., J. G. Tian, Z. Guo, D. M. Ren, F. Du, J. Y. Zheng and Y. S. Chen (2008). Enhanced Optical Limiting Effects in Porphyrin-Covalently Functionalized Single-Walled Carbon Nanotubes. *Advanced Materials*, Vol. 20, No. 3, pp. 511-515.

Liu, Z. B., Y. Wang, X. L. Zhang, Y. F. Xu, Y. S. Chen and J. G. Tian (2009). Nonlinear optical properties of graphene oxide in nanosecond and picosecond regimes. *Applied Physics Letters*, Vol. 94, No. 2, pp. 021902.

Liu, Z. B., Y. F. Xu, X. Y. Zhang, X. L. Zhang, Y. S. Chen and J. G. Tian (2009). Porphyrin and Fullerene Covalently Functionalized Graphene Hybrid Materials with Large Nonlinear Optical Properties. *Journal of Physical Chemistry B*, Vol. 113, No. 29, pp. 9681-9686.

Loh, K. P., Q. L. Bao, G. Eda and M. Chhowalla (2010). Graphene oxide as a chemically tunable platform for optical applications. *Nature Chemistry*, Vol. 2, No. 12, pp. 1015-1024.

Lotya, M., Y. Hernandez, P. J. King, R. J. Smith, V. Nicolosi, L. S. Karlsson, F. M. Blighe, S. De, Z. M. Wang, I. T. McGovern, G. S. Duesberg and J. N. Coleman (2009). Liquid Phase Production of Graphene by Exfoliation of Graphite in Surfactant/Water Solutions. *Journal of the American Chemical Society*, Vol. 131, No. 10, pp. 3611-3620.

Mamidala, V., L. Polavarapu, J. Balapanuru, K. P. Loh, Q.-H. Xu and W. Ji (2010). Enhanced nonlinear optical responses in donor-acceptor ionic complexes via photo induced energy transfer. *Optics Express*, Vol. 18, No. 25, pp. 25928-25935.

Mansour, K., M. J. Soileau and E. W. Van Stryland (1992). Nonlinear optical properties of carbon-black suspensions (ink). *Journal of the Optical Society of America B-Optical Physics*, Vol. 9, No. 7, pp. 1100-1109.

Midya, A., V. Mamidala, J. X. Yang, P. K. L. Ang, Z. K. Chen, W. Ji and K. P. Loh (2010). Synthesis and Superior Optical-Limiting Properties of Fluorene-Thiophene-Benzothiadazole Polymer-Functionalized Graphene Sheets. *Small*, Vol. 6, No. 20, pp. 2292-2300.

Nair, R. R., P. Blake, A. N. Grigorenko, K. S. Novoselov, T. J. Booth, T. Stauber, N. M. R. Peres and A. K. Geim (2008). Fine structure constant defines visual transparency of graphene. *Science*, Vol. 320, No. 5881, pp. 1308-1308.

Ni Mhuircheartaigh, E. M., S. Giordani and W. J. Blau (2006). Linear and nonlinear optical characterization of a tetraphenylporphyrin-carbon nanotube composite system. *Journal of Physical Chemistry B*, Vol. 110, No. 46, pp. 23136-23141.

Niu, L., P. Li, Y. Chen, J. Wang, J. Zhang, B. Zhang and W. J. Blau (2011). Conjugated polymer covalently modified multiwalled carbon nanotubes for optical limiting. *Journal of Polymer Science Part A: Polymer Chemistry*, Vol. 49, No. 1, pp. 101-109.

Novoselov, K. S., A. K. Geim, S. V. Morozov, D. Jiang, M. I. Katsnelson, I. V. Grigorieva, S. V. Dubonos and A. A. Firsov (2005). Two-dimensional gas of massless Dirac fermions in graphene. *Nature*, Vol. 438, No. 7065, pp. 197-200.

Novoselov, K. S., A. K. Geim, S. V. Morozov, D. Jiang, Y. Zhang, S. V. Dubonos, I. V. Grigorieva and A. A. Firsov (2004). Electric field effect in atomically thin carbon films. *Science*, Vol. 306, No. 5696, pp. 666-669.

Novoselov, K. S., D. Jiang, F. Schedin, T. J. Booth, V. V. Khotkevich, S. V. Morozov and A. K. Geim (2005). Two-dimensional atomic crystals. *Proceedings of the National Academy of Sciences of the United States of America*, Vol. 102, No. 30, pp. 10451-10453.

O'Flaherty, S. A., R. Murphy, S. V. Hold, M. Cadek, J. N. Coleman and W. J. Blau (2003). Material investigation and optical limiting properties of carbon nanotube and nanoparticle dispersions. *Journal of Physical Chemistry B*, Vol. 107, No. 4, pp. 958-964.

O'Flaherty, S. M., J. J. Doyle and W. J. Blau (2004). Numerical approach for optically limited pulse transmission in polymer-phthalocyanine composite systems. *Journal of Physical Chemistry B*, Vol. 108, No. 45, pp. 17313-17319.

O'Flaherty, S. M., S. V. Hold, M. E. Brennan, M. Cadek, A. Drury, J. N. Coleman and W. J. Blau (2003). Nonlinear optical response of multiwalled carbon-nanotube dispersions. *Journal of the Optical Society of America B-Optical Physics*, Vol. 20, No. 1, pp. 49-58.

O'Flaherty, S. M., S. V. Hold, M. J. Cook, T. Torres, Y. Chen, M. Hanack and W. J. Blau (2003). Molecular engineering of peripherally and axially modified phthalocyanines for optical limiting and nonlinear optics. *Advanced Materials*, Vol. 15, No. 1, pp. 19-32.

Rayfield, G. W., A. Sarkar, S. Rahman, J. P. Godschalx and E. W. Taylor (2010). Mechanistic studies for optical switching materials for space environments. *Nanophotonics and Macrophotonics for Space Environments Iv*. E. W. Taylor and D. A. Cardimona. Bellingham, Spie-Int Soc Optical Engineering. 7817.

Senge, M. O., M. Fazekas, E. G. A. Notaras, W. J. Blau, M. Zawadzka, O. B. Locos and E. M. N. Mhuircheartaigh (2007). Nonlinear optical properties of porphyrins. *Advanced Materials*, Vol. 19, No. 19, pp. 2737-2774.

Sun, X., R. Q. Yu, G. Q. Xu, T. S. A. Hor and W. Ji (1998). Broadband optical limiting with multiwalled carbon nanotubes. *Applied Physics Letters*, Vol. 73, No. 25, pp. 3632-3634.

Sun, Y. P. and J. E. Riggs (1999). Organic and inorganic optical limiting materials. From fullerenes to nanoparticles. *International Reviews in Physical Chemistry*, Vol. 18, No. 1, pp. 43-90.

Sun, Z. P., T. Hasan, F. Torrisi, D. Popa, G. Privitera, F. Q. Wang, F. Bonaccorso, D. M. Basko and A. C. Ferrari (2010). Graphene Mode-Locked Ultrafast Laser. *Acs Nano*, Vol. 4, No. 2, pp. 803-810.

Tutt, L. W. and T. F. Boggess (1993). A review of optical limiting mechanisms and devices using organics, fullerenes, semiconductors and other materials. *Progress in Quantum Electronics*, Vol. 17, No. 4, pp. 299-338.

Tutt, L. W. and A. Kost (1992). Optical Limiting Performance of C60 and C70 Solutions. *Nature*, Vol. 356, No. 6366, pp. 225-226.

Venkatram, N., D. N. Rao and M. A. Akundi (2005). Nonlinear absorption, scattering and optical limiting studies of CdS nanoparticles. *Optics Express*, Vol. 13, No. 3, pp. 867-872.

Vivien, L., E. Anglaret, D. Riehl, F. Bacou, C. Journet, C. Goze, M. Andrieux, M. Brunet, F. Lafonta, P. Bernier and F. Hache (1999). Single-wall carbon nanotubes for optical limiting. *Chemical Physics Letters*, Vol. 307, No. 5-6, pp. 317-319.

Vivien, L., P. Lancon, D. Riehl, F. Hache and E. Anglaret (2002). Carbon nanotubes for optical limiting. *Carbon*, Vol. 40, No. 10, pp. 1789-1797.

Vivien, L., J. Moreau, D. Riehl, P. A. Allonclе, M. Autric, F. Hache and E. Anglaret (2002). Shadowgraphic imaging of carbon nanotube suspensions in water and in chloroform. *Journal of the Optical Society of America B-Optical Physics*, Vol. 19, No. 11, pp. 2665-2672.

Vivien, L., D. Riehl, F. Hache and E. Anglaret (2000). Nonlinear scattering origin in carbon nanotube suspensions. *Journal of Nonlinear Optical Physics & Materials*, Vol. 9, No. 3, pp. 297-307.

Wang, J. and W. J. Blau (2008). Linear and nonlinear spectroscopic studies of phthalocyanine-carbon nanotube blends. *Chemical Physics Letters*, Vol. 465, No. 4-6, pp. 265-271.

Wang, J. and W. J. Blau (2008). Nonlinear optical and optical limiting properties of individual single-walled carbon nanotubes. *Applied Physics B-Lasers and Optics*, Vol. 91, No. 3-4, pp. 521-524.

Wang, J. and W. J. Blau (2008). Solvent effect on optical limiting properties of single-walled carbon nanotube dispersions. *Journal of Physical Chemistry C*, Vol. 112, No. 7, pp. 2298-2303.

Wang, J. and W. J. Blau (2009). Inorganic and Hybrid Nanostructures for Optical Limiting. *Journal of Optics A – Pure and Applied Optics*, Vol. 11, No. 2, pp. 024001.

Wang, J., Y. Chen and W. J. Blau (2009). Carbon Nanotubes and Nanotube Composites for Nonlinear Optical Devices. *Journal of Materials Chemistry*, Vol. 19, No. 40, pp. 7425-7443.

Wang, J., D. Früchtl and W. J. Blau (2010). The importance of solvent properties for optical limiting of carbon nanotube dispersions. *Optics Communications*, Vol. 283, No. 3, pp. 464-468.

Wang, J., D. Früchtl, Z. Sun, J. N. Coleman and W. J. Blau (2010). Control of Optical Limiting of Carbon Nanotube Dispersions by Changing Solvent Parameters. *The Journal of Physical Chemistry C*, Vol. 114, No. 13, pp. 6148-6156.

Wang, J., Y. Hernandez, M. Lotya, J. N. Coleman and W. J. Blau (2009). Broadband Nonlinear Optical Response of Graphene Dispersions. *Advanced Materials*, Vol. 21, No. 23, pp. 2430-2435.

Webster, S., M. Reyes-Reyes, X. Pedron, R. López-Sandoval, M. Terrones and D. L. Carroll (2005). Enhanced nonlinear transmittance by complementary nonlinear mechanisms: a reverse-saturable absorbing dye blended with nonlinear-scattering carbon nanotubes. *Advanced Materials*, Vol. 17, No. 10, pp. 1239-1243.

Xia, Y., P. Yang, Y. Sun, Y. Wu, B. Mayers, B. Gates, Y. Yin, F. Kim and H. Yan (2003). One-Dimensional Nanostructures: Synthesis, Characterization, and Applications. *Advanced Materials*, Vol. 15, No. 5, pp. 353-389.

Xu, Y., Z. Liu, X. Zhang, Y. Wang, J. Tian, Y. Huang, Y. Ma, X. Zhang and Y. Chen (2009). A Graphene Hybrid Material Covalently Functionalized with Porphyrin: Synthesis and Optical Limiting Property. *Advanced Materials*, Vol. 21, No. 12, pp. 1275-1279.

Zhang, B., J. Wang, Y. Chen, D. Fruchtl, B. Yu, X. D. Zhuang, N. He and W. J. Blau (2010). Multiwalled Carbon Nanotubes Covalently Functionalized with Poly(N-vinylcarbazole) via RAFT Polymerization: Synthesis and Nonlinear Optical Properties. *Journal of Polymer Science Part a-Polymer Chemistry*, Vol. 48, No. 14, pp. 3161-3168.

Zhang, X. L., X. Zhao, Z. B. Liu, Y. S. Liu, Y. S. Chen and J. G. Tian (2009). Enhanced nonlinear optical properties of graphene-oligothiophene hybrid material. *Optics Express*, Vol. 17, No. 26, pp. 23959-23964.

Zhang, X. Y., Z. B. Liu, Y. Huang, X. J. Wan, J. G. Tian, Y. F. Ma and Y. S. Chen (2009). Synthesis, Characterization and Nonlinear Optical Property of Graphene-C-60 Hybrid. *Journal of Nanoscience and Nanotechnology*, Vol. 9, No. 10, pp. 5752-5756.

Zhang, X. Y., X. Y. Yang, Y. F. Ma, Y. Huang and Y. S. Chen (2010). Coordination of Graphene Oxide with Fe3O4 Nanoparticles and Its Enhanced Optical Limiting Property. *Journal of Nanoscience and Nanotechnology*, Vol. 10, No. 5, pp. 2984-2987.

Zhao, B. S., B. B. Cao, W. L. Zhou, D. Li and W. Zhao (2010). Nonlinear Optical Transmission of Nanographene and Its Composites. *Journal of Physical Chemistry C*, Vol. 114, No. 29, pp. 12517-12523.

Zheng, C., M. Feng and H. B. Zhan (2010). The synthesis of carbon nanotube based composites with conducting, semiconducting, and insulating coatings and their optical limiting properties. *Carbon*, Vol. 48, No. 13, pp. 3750-3759.

Zhou, Y., Q. L. Bao, L. A. L. Tang, Y. L. Zhong and K. P. Loh (2009). Hydrothermal Dehydration for the "Green" Reduction of Exfoliated Graphene Oxide to Graphene and Demonstration of Tunable Optical Limiting Properties. *Chemistry of Materials*, Vol. 21, No. 13, pp. 2950-2956.

Zhu, J., Y. Li, Y. Chen, J. Wang, B. Zhang, J. Zhang and W. J. Blau (2011). Graphene oxide covalently functionalized with zinc phthalocyanine for broadband optical limiting. *Carbon*, Vol. 49, No. 6, pp. 1900–1905.